Store-and-forward based methods for the signal control problem in large-scale congested urban road networks

K. Aboudolas *, M. Papageorgiou, E. Kosmatopoulos

Dynamic Systems and Simulation Laboratory,

Technical University of Crete, GR-73100 Chania, Greece

Abstract

The problem of designing network-wide traffic signal control strategies for large-scale congested urban road networks is considered. One known and two novel methodologies, all based on the store-and-forward modeling paradigm, are presented and compared. The known methodology is a linear multivariable feedback regulator derived through the formulation of a linear-quadratic optimal control problem. An alternative, novel methodology consists of an open-loop constrained quadratic optimal control problem, whose numerical solution is achieved via quadratic programming. Yet a different formulation leads to an open-loop constrained nonlinear optimal control problem, whose numerical solution is achieved by use of a feasible-direction algorithm. A preliminary simulation-based investigation of the signal control problem for a large-scale urban road network using these methodologies demonstrates the comparative efficiency and real-time feasibility of the developed signal control methods.

Key words: Traffic signal control, traffic congestion, store-and-forward modeling, control methods in transportation systems

* Corresponding author. Tel.:+30-28210-37289; Fax:+30-28210-37584

Email addresses: aboud@dssl.tuc.gr (K. Aboudolas), markos@dssl.tuc.gr (M. Papageorgiou), kosmatop@dssl.tuc.gr (E. Kosmatopoulos).

1 Introduction

In view of the increasing traffic congestion and lack of possibilities for infrastructure expansion in urban road networks, the importance of efficient signal control strategies, particularly under saturated traffic conditions, can hardly be overemphasized. It is generally believed that real-time systems responding automatically to the prevailing traffic conditions, are potentially more efficient than clock-based fixed-time control settings, possibly extended via a simple traffic-actuated logic.

On the other hand, the development of optimal network-wide real-time signal control strategies using detailed network models is deemed computationally infeasible due to the discrete nature of the related optimization problem that leads to exponentially increasing complexity (see e.g. Papageorgiou et al., 2003); as a consequence, the developed or implemented real-time signal control strategies must include simplifications or heuristics, some of which may render the strategies less efficient under saturated traffic conditions. A particular simplified control design avenue pursued by various works in the past is based on the store-and-forward modeling (SFM) paradigm; a particular advantage of these approaches is that they are applicable to large-scale congested networks; their main disadvantage is that, due to the particular modeling simplification employed, they are only applicable for split optimization, while cycle time and offsets must be delivered by other algorithms.

This paper presents and compares one known and two novel network-wide signal control methodologies based on SFM. More specifically, a generic mathematical model, based on the store-and-forward modeling paradigm, for the traffic flow process in large-scale urban networks is presented first. Three modeling variations lead to the three alternative optimal control methodologies for the design of signal control strategies that aim at minimizing and balancing the link queues so as to reduce the risk of queue spillback under saturated

traffic conditions. Based on the three control methodologies, signal control plans (splits) may be computed in real time (once per cycle) through a linear multivariable feedback regulator (LQ), an open-loop constrained quadratic optimal control problem (QPC), or an open-loop constrained nonlinear optimal control problem (NOC), respectively. In order to evaluate the comparative results and real-time feasibility of the proposed methods, a preliminary comparison of the closed-loop behaviour of the linear multivariable regulator with the open-loop behaviour of QPC and NOC methodologies, is carried out.

2 Background

A variety of real-time traffic signal control strategies for urban networks has been developed during the past few decades. Without attempting a survey of this vast research area we will address a few selected strategies (for an up-to-date account we refer the reader to Papageorgiou et al. (2003)), some of which have been implemented in real-life conditions while others are still in the research and development stage. We may distinguish two principal classes of signal control strategies. In the first class, strategies are only applicable to (or efficient for) networks with undersaturated traffic conditions, whereby all queues at the signalized junctions are served during the next green phase. In the second class, we have strategies applicable to networks with oversaturated traffic conditions, whereby queues may grow in some links with an imminent risk of spillback and eventually even of gridlock in network cycles.

SCOOT (Hunt et al., 1982; Bretherton et al., 2004) and SCATS (Lowrie, 1982) are two well-known and widely used coordinated traffic-responsive strategies that function effectively when the traffic conditions in the network are below saturation, but their performance may deteriorate when severe congestion persists during the peak period. Other elaborated model-based traffic-responsive strategies such as PRODYN (Farges et al., 1983)

and RHODES (Mirchandani and Head, 1998; Mirchandani and Wang, 2005) employ dynamic programming while OPAC (Gartner, 1983) employs exhaustive enumeration. Due to the exponential complexity of these solution algorithms, the basic optimization kernel is not real-time feasible for more than one junction.

Store-and-forward modeling of traffic networks was first suggested by Gazis and Potts (1963) and has since been used in various works notably for road traffic control. This modeling approach that describes the network traffic flow process in a simplified way, so as to circumvent the inclusion of discrete variables, offers a major advantage: it allows for highly efficient optimization and control methods with polynomial complexity to be used for the coordinated control of large-scale congested urban networks. On the other hand, the introduced modeling simplification allows only for split optimization, while cycle time and offsets must be delivered by other control algorithms. A recently developed signal control strategy of this type is TUC (Diakaki et al., 2002) that will be outlined later.

More recently, a number of approaches have been proposed employing various computationally expensive numerical solution algorithms, including genetic algorithms (Abu-Lebdeh and Benekohal, 1997; Lo et al., 2001), multi-extended linear complementary programming (Schutter and Moor, 1998), and mixed-integer linear programming (Lo, 1999; Beard and Ziliaskopoulos, 2006). In Lo (1999); Lo et al. (2001); Beard and Ziliaskopoulos (2006) the traffic flow conditions are modeled using the cell transmission model (Daganzo, 1994), a convergent numerical approximation to the first-order hydrodynamic model of traffic flow for network links. In view of the high computational requirements, the real-life implementation of these optimization-based approaches might face some difficulties in terms of real-time feasibility.

3 Store-and-forward modeling

The urban road network is represented as a directed graph with links $z \in Z$ and junctions $j \in J$. For each signalized junction j, we define the sets of incoming I_j and outgoing O_j links. It is assumed that the offset and the cycle time C_j of junction j are fixed or calculated in real time by another algorithm. In addition, to enable network offset coordination within the present setting, we assume that $C_j = C$ for all junctions $j \in J$, which is a quite usual assumption. Furthermore, the signal control plan of junction j (including the fixed lost time L_j) is based on a fixed number of stages that belong to the set F_j, while v_z denotes the set of stages where link z has right of way (r.o.w.). Finally, the saturation flow S_z of link $z \in Z$, and the turning rates $t_{w,z}$, where $w \in I_j$ and $z \in O_j$, are assumed to be known and constant for LQ control but may be time-varying for the QPC and NOC approaches.

By definition, the constraint

$$\sum_{i \in F_j} g_{j,i} + L_j = (\text{or } \leq)\, C \tag{1}$$

holds at each junction j, where $g_{j,i}$, is the green time of stage i at junction j. Inequality in (1) may be useful in cases of strong network congestion to allow for all-red stages. In addition, the constraint

$$g_{j,i} \geq g_{j,i,\min}, \quad i \in F_j \tag{2}$$

where $g_{j,i,\min}$ is the minimum permissible green time for stage i at junction $j \in J$, is introduced to guarantee allocation of sufficient green time to pedestrian phases.

Consider a link z connecting two junctions M and N such that $z \in O_M$ and $z \in I_N$

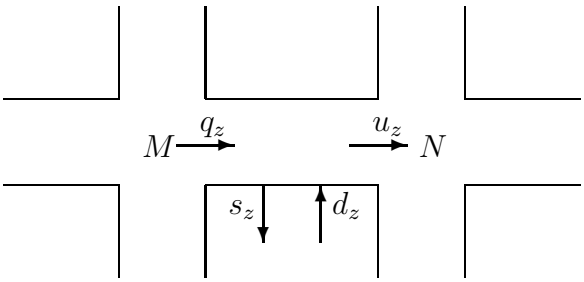

Fig. 1. An urban road link.

(Fig. 1). The dynamics of link z are given by the conservation equation

$$x_z(k+1) = x_z(k) + T\Big[q_z(k) - s_z(k) + d_z(k) - u_z(k)\Big] \tag{3}$$

where $x_z(k)$ is the number of vehicles within link z (for the sake of brevity sometimes called queues in the following) at time kT, $q_z(k)$ and $u_z(k)$ are the inflow and outflow, respectively, of link z in the sample period $[kT, (k+1)T]$; T is the discrete time step and $k = 0, 1, \ldots$ the discrete time index; d_z and s_z are the demand and the exit flow within the link, respectively. For the exit flow we set $s_z(k) = t_{z,0} q_z(k)$, where the exit rates $t_{z,0}$ are assumed to be known.

Queues are subject to the constraints

$$0 \leq x_z(k) \leq x_{z,\max}, \quad \forall\, z \in Z \tag{4}$$

where $x_{z,\max}$ is the maximum admissible queue length. This constraint may automatically lead to a suitable upstream gating in order to protect downstream areas from oversaturation during periods of high demand.

The inflow to the link z is given by $q_z(k) = \sum_{w \in I_M} t_{w,z} u_w(k)$, where $t_{w,z}$ with $w \in I_M$ are the turning rates towards link z from the links that enter junction M.

We now introduce a critical simplification for the outflow u_z that characterizes the utilized

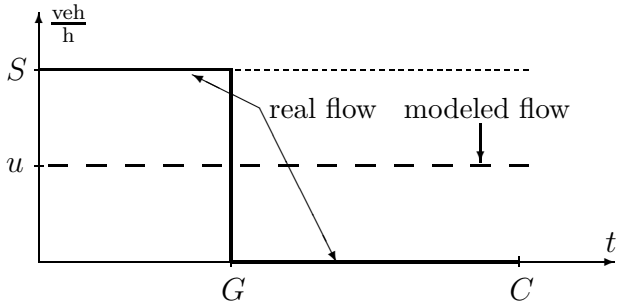

Fig. 2. Simplified modeling of link outflow.

modeling approach. Provided that space is available in the downstream links and that x_z is sufficiently high (which are surveilled by constraint (4)), the outflow (real flow) u_z of link z is equal to the saturation flow S_z if the link has r.o.w., and equal to zero otherwise. However, if the discrete time step T is equal to C, an average value for each period (modeled flow) is obtained (Fig. 2) by

$$u_z(k) = G_z(k)S_z/C \tag{5}$$

where G_z, is the green time of link z, calculated as $G_z(k) = \sum_{i \in v_z} g_{j,i}(k)$. The consequences of this simplification for the derived signal control strategies are discussed further below.

Replacing (5) in (3) for all z and organizing all resulting equations in one single vector-based equation leads to a linear state-space model for road networks of arbitrary size, topology, and characteristics which is given by

$$\mathbf{x}(k+1) = \mathbf{x}(k) + \mathbf{B}\mathbf{g}(k) + T\mathbf{d}(k) \tag{6}$$

where $\mathbf{x}(k)$ is the state vector (consisting of the number of vehicles x_z of each link z); $\mathbf{g}(k)$ is the control vector (consisting of all the green times $g_{j,i}$); $\mathbf{d}(k)$ is the disturbance vector (consisting of the demand flows d_z of each link z); $\mathbf{B}$ results from (3), (5) as a constant matrix of appropriate dimensions containing the network characteristics (topology, saturation flows, turning rates).

As a consequence of simplification (5), i.e. due to the model time step T being equal to the cycle time C, the model is not aware of short-term queue oscillations due to green-red switchings within a cycle; in other words, the model describes a continuous (uninterrupted) average outflow from each network link (as long as there is sufficient demand upstream and sufficient space downstream). Moreover, offset and cycle time have no impact within the SFM and must be either fixed or updated in real time independently (Diakaki et al., 2003). These consequences of simplification (5) is the price to pay for avoiding the explicit modeling of intra-cycle red-green switchings which would render the resulting optimization problem discrete (combinatorial) and would lead to exponential increase of computational complexity for its exact solution as in several previous works.

Note that the SFM (6) is simpler than the cell transmission model (CTM) employed in some previous works (Lo et al., 2001; Lo, 1999; Beard and Ziliaskopoulos, 2006). In fact, the CTM calls for subdivision of network links into shorter segments (cells) and correspondingly shorter time steps T of 5 s or less. Thus the CTM describes the (inhomogeneous) link-internal traffic state more accurately than the SFM. However, the more accurate description of link-internal traffic flow dynamics has a limited significance in interrupted (signal-controlled) traffic network flow, in contrast to the uninterrupted freeway traffic flow. Moreover, real-time application of a CTM-based control strategy would call for specific measurements (or estimates) for each cell which are usually not available in current network control infrastructures.

The most suited control objective under congested traffic conditions is to minimize the risk of oversaturation and spillback of link queues. To this end, one may attempt to minimize and balance the links' relative occupancies $x_z/x_{z,\max}$. This criterion is physically reasonable as well as convenient from the numerical solution point of view, as we will see later. Alternatively, one may minimize the total time spent (which corresponds to minimization of the sum of x_z) but this would lead to a linear programming problem with

vertex solutions (e.g. $x_z = 0$ for some links and $x_z = x_{z,\max}$ for others) that may increase the risk of link queue spillback.

4 Control and optimization approaches

4.1 Linear-quadratic (LQ) optimal control

A first approach towards network-wide real-time signal control based on the SFM (6) is derived as follows. We assume availability of a network-wide fixed signal control plan $\mathbf{g}^N$ that may have been calculated by use of any fixed-time control method based on fixed (historical) demands $\mathbf{d}^N$. We also assume that, under the demand $\mathbf{d}^N$, the signal controls $\mathbf{g}^N$ lead to non-saturated network traffic conditions, i.e. to a constant state $\mathbf{x}^N$. Based on (6), it is easy to see that these assumptions imply $\mathbf{B}\mathbf{g}^N + T\mathbf{d}^N = \mathbf{0}$. We now define the control and demand deviations $\Delta\mathbf{g}(k) = \mathbf{g}(k) - \mathbf{g}^N$ and $\Delta\mathbf{d}(k) = \mathbf{d}(k) - \mathbf{d}^N$, respectively, which yield from (6)

$$\mathbf{x}(k+1) = \mathbf{x}(k) + \mathbf{B}\Delta\mathbf{g}(k) + T\Delta\mathbf{d}(k). \tag{7}$$

A quadratic criterion that addresses adequately the control objective mentioned in Section 3 has the general form

$$\mathcal{J} = \sum_{k=0}^{\infty} \left(\|\mathbf{x}(k)\|^2_{\mathbf{Q}} + \|\Delta\mathbf{g}(k)\|^2_{\mathbf{R}} \right) \tag{8}$$

where $\mathbf{Q}$ and $\mathbf{R}$ are nonnegative definite, diagonal weighting matrices with appropriate dimensions. The diagonal elements of $\mathbf{Q}$ are set equal to $1/x_{z,\max}$ in order to minimize and balance the relative occupancies of the network links. Furthermore, the magnitude of the control reactions can be influenced by the choice of the weighting matrix $\mathbf{R} = r\mathbf{I}$ where $\mathbf{I}$ is the unit maxtrix. To this end, the choice of r may be performed via a trial-and-error procedure (e.g. using simulation, see Diakaki (1999)). The trial-and-error

procedure consists in fixing some r-values; simulating the corresponding control results for representative demand scenarios; evaluating the obtained sub-criteria values; so as to achieve a satisfactory control behaviour for a given application network. The trial-and-error procedure may even be omitted because the control results are little sensitive for a broad range of (usually very low) r values (Diakaki, 1999).

Minimization of the cost criterion (8) subject to (7) (assuming $\Delta\mathbf{d}(k) = \mathbf{0}$ as it is usual for LQ control) leads to a linear multivariable feedback regulator given by

$$\mathbf{g}(k) = \mathbf{g}^N - \mathbf{L}\mathbf{x}(k) \tag{9}$$

where the feedback gain matrix $\mathbf{L}$ results as a straightforward solution of the corresponding algebraic Riccati equation. Note that, according to the LQ control theory, the gain matrix $\mathbf{L}$ is constant thanks to the selection of an infinite time-horizon in the control objective (8); it should also be noted that $\mathbf{g}^N$ in (9) may be time-varying if there is a need for this, while $\mathbf{d}^N$ is not actually needed in the LQ control application.

Essentially, the regulator (9) modifies in real time the fixed plan $\mathbf{g}^N$ appropriately, to respond to the formation of queues $\mathbf{x}(k)$ in the network links. Sufficiently reliable estimates of $x_z(k)$ may be obtained on the basis of one single occupancy-measuring detector cross-section, preferably in the middle of the link, see Diakaki (1999), for details. This is the multivariable regulator approach taken by the signal control strategy TUC (Diakaki et al., 2002) to calculate in real time the network splits, while cycle time and offset are calculated by other parallel algorithms (Diakaki et al., 2003). TUC has been successfully field-implemented in large networks of 5 cities in 4 different countries, see Kosmatopoulos et al. (2006), for recent field results.

Note that the LQ control theory does not allow for direct consideration of the constraints

(1) and (2). For this reason, a suitable real-valued quadratic knapsack algorithm is used after the application of (9) in order to suitably modify the calculated $g_{j,i}$ green times of each junction so as to satisfy the constraints (1) and (2). More specifically, the knapsack algorithm for each junction j reads: For given $g_{j,i}$ (resulting from (9)), find the modified green times $\tilde{g}_{j,i}$, $\forall i \in F_j$, that minimize

$$\Phi(\tilde{g}_{j,i}) = \frac{1}{2} \sum_{i \in F_j} \left(\tilde{g}_{j,i} - g_{j,i}\right)^2 / g_{j,i} \tag{10}$$

subject to (1), (2). It may be readily shown that the minimization of (10) subject to (1) alone would lead to a solution that satisfies $\tilde{g}_{j,i}/g_{j,i} = \tilde{g}_{j,l}/g_{j,l}$ $\forall\,(i,l)$, i.e. the modified $\tilde{g}_{j,i}$ would preserve the same splits as $g_{j,l}$ along with satisfying (1). The above real-valued quadratic knapsack problem approximates this solution to the extent allowed by the additional constraint (2). The exact numerical solution of a real-valued quadratic knapsack problem is known (Helgason et al., 1980; Diakaki, 1999) to call for at most as many iterations as the number of involved variables, which, in our case, hardly exceeds 3 or 4 stages at each junction.

The main advantage of the LQ approach to network-wide signal control is the simplicity of required real-time calculations, thanks to the closed-loop solution (9) of the formulated optimal control problem which circumvents the need for numerical solution of an optimization problem in real-time. In fact, the real-time application of the LQ method calls for one measurement/estimation of $\mathbf{x}(k)$ per cycle, based on which the control strategy executes the control law (9), applies the constraints based on (10) and returns the green times $\mathbf{g}(k)$ for application in the next cycle.

A potential disadvantage of the LQ approach is the a posteriori application of the constraints (1), (2), which may lead to suboptimal solutions; this is a first motivation for the development of more complex, but potentially more efficient approaches that will be

presented in the next sections.

It should also be stressed that the LQ strategy does not consider explicitly the queue constraints (4). Although the balancing of the link queues via the control objective (8) reduces the risk of overspilling links in an indirect way, it is interesting to consider more complex approaches that account for the queue constraints (4) strictly as in the following sections.

4.2 Open-loop quadratic-programming control (QPC)

In contrast to other SFM-based approaches (see for instance Singh and Tamura (1974)), we will now introduce the green times G_z of each link z as additional independent variables. The reason behind this modification is that we want to increase the control flexibility and potential efficiency while explicitly considering the queue constraints (4) (Papageorgiou, 1995). The introduced link green times G_z are constrained as follows:

$$0 \leq G_z(k) \leq \sum_{i \in v_z} g_{j,i}(k), \quad \forall\, j \in J. \tag{11}$$

In more detail, the reason for introducing independent G_z in the problem formulation may be illustrated via the following observation: if the queue x_z is not sufficiently long or even zero; or if the downstream link queue is too long to accommodate a high inflow; then the constraints (4) will become active and will reduce the corresponding stage greens accordingly. As an illustrative example, assume that at a certain cycle there are two links z and w having r.o.w. simultaneously during a stage (M, i), and that $x_z \approx 0$ while $x_w \gg 0$ (Fig. 3). If G_z and G_w are not independently introduced, we have by definition $G_z = G_w = g_{M,i}$. Then, the stage green $g_{M,i}$ will be strictly limited by the constraint $x_z \geq 0$ although link w may need a longer green phase for dissolving x_w. In contrast, by

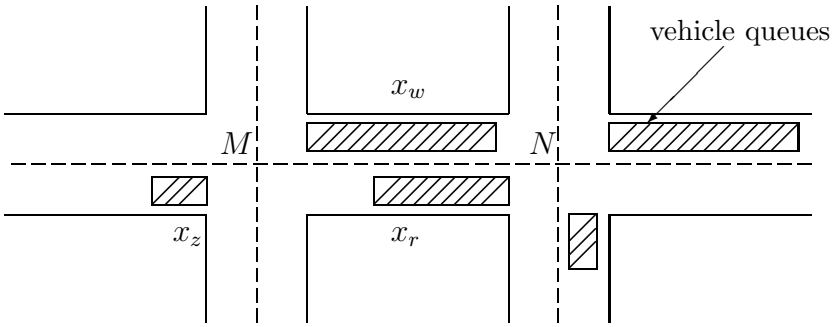

Fig. 3. A two-way link connecting two junctions M and N.

introducing G_z and G_w independently, the algorithm can guarantee $x_z \geq 0$ by choosing G_z accordingly short without constraining G_w and the stage green. Similarly, if the link r downstream of link z is close to spillback (see Fig. 3), the constraint $x_r \leq x_{r,\max}$ can be guaranteed by choosing G_z accordingly short without constraining the green time of other links that are having r.o.w. during the same stage.

In view of the above modification, replacing (5) in (3) leads to a linear state-space model for road networks of arbitrary size, topology, and characteristics

$$\mathbf{x}(k+1) = \mathbf{x}(k) + \overline{\mathbf{B}}(k)\mathbf{G}(k) + T\mathbf{d}(k) \tag{12}$$

where $\mathbf{G}(k)$ is the link control vector with elements the green times G_z of each link z; $\overline{\mathbf{B}}$ is a matrix of appropriate dimensions reflecting the network characteristics. Note that in this approach $\overline{\mathbf{B}}$ may be time-variant, if the involved saturation flows or turning rates are time-variant.

In this approach, the employed finite-horizon quadratic criterion that addresses the stated control objective has the form

$$\mathcal{J} = \sum_{k=0}^{K} \sum_{z \in Z} \frac{x_z^2(k)}{x_{z,\max}}. \tag{13}$$

Note that this criterion is identical with the criterion (8) for $K \to \infty$, $r = 0$. Note also that model (12), with independent G_z for each link, could also be used within the LQ

approach of Section 4.1.

On the basis of the linear model (12), the constraints (1), (2), (4), plus the constraint (11) and the quadratic cost criterion (13), a (dynamic) optimal control problem may be formulated over a finite time-horizon K, starting with the known initial state $\mathbf{x}(0)$ in the state equation (12).

In summary, the optimization problem has three types of time-dependent variables, namely the stage green times $g_{j,i}(k)$, the state variables $x_z(k)$, and the link green times $G_z(k)$. This QP problem (with very sparse matrices) may be readily solved by use of broadly available codes or commercial software within few CPU-seconds even for large-scale networks and long time-horizons.

4.3 Open-loop nonlinear optimal control (NOC)

4.3.1 Model overview

In this design approach, we re-introduce the link outflow $u_z(k)$ into our problem and recall that the outflow is given by (5) only under the assumption that $x_z(k)$ satisfies the constraints (4). Instead of (5), we now define a nonlinear outflow function that models the intra-cycle traffic flow process more accurately. More precisely, we assume that the model's time step is $T \ll C$ while the control time step T_c remains equal to C, i.e. control decisions are taken at each cycle as in previous methods. Then the outflow $u_z(k)$ is given by

$$u_z(k) = \begin{cases} 0 & \text{if any } x_{d,z}(k) \geq c x_{d,\max} \\ \min\left\{\frac{x_z(k)}{T}, \frac{G_z(\kappa) S_z}{C}\right\} & \text{else} \end{cases} \tag{14}$$

where d is a downstream link of link z with turning rate $t_{z,d} \neq 0$, and we have the parameter $c \in (0, 1]$; note that k is now the model discrete time index (with time step

$T \ll C$) while κ is the control discrete time index (with time step $T_\mathrm{c} = C$). By introducing (14), the state variables are allowed to change their value more frequently than the control variables. More precisely, typical discrete-time model steps T for the traffic flow model (3) using (14) may be in the order of 5 s while the control variables change their value in discrete-time control steps T_c, e.g. at each cycle. Note that, when using (14), the queue constraints (4) are considered indirectly and may hence be dropped; indeed the link outflow in (14) becomes zero if there is no vehicle in the link or if a downstream link is full. Note also that the basic simplification of SFM, i.e. a continuous link outflow (rather than zero flow during red and free flow during green), is still maintained in this approach. The introduction of (14) instead of (4) and (5) improves the model accuracy within cycles but leads to a more complex (nonlinear) model due to the switching rule in (14).

Replacing (14) in (3) we obtain a nonlinear state-space model for road networks of arbitrary size, topology, and characteristics (Aboudolas, 2003)

$$\mathbf{x}(k+1) = \mathbf{f}\Big[\mathbf{x}(k), \mathbf{g}(\kappa), \mathbf{d}(k)\Big], \quad \kappa = [k/\tau] \tag{15}$$

where $\mathbf{f}$ is a nonlinear vector function, κ is a discrete-time index of the control variables, $T_\mathrm{c} = \tau T$ while $[\eta]$ denotes the integer part of η.

The cost criterion in a nonlinear optimal control problem may have any arbitrary nonlinear form. In the particular case the chosen cost criterion to be minimized has the form

$$\mathcal{J} = \sum_{z \in Z} \frac{x_z^2(K)}{x_{z,\max}} + \sum_{k=0}^{K-1} \left\{ \sum_{z \in Z} \frac{x_z^2(k)}{x_{z,\max}} + a_\mathrm{f} \sum_{j=1}^{|J|} \sum_{i=1}^{|F_j|} \Big[g_{j,i}(\kappa) - g_{j,i}(\kappa - 1) \Big]^2 \right\} \tag{16}$$

where a_f is a positive weighting factor. This criterion, excluding the last penalty term, attempts the minimization and balance of the links' relative occupancies $x_z/x_{z,\max}$ similarly

to (13) and (8); in fact for $a_{\mathrm{f}} = 0$, (16) becomes identical with (13). The penalty term is included in the cost criterion so that possible high-frequency oscillations of the control trajectories be suppressed. The weight a_{f} may be adjusted via trial-and-error, striking a balance between acceptable time-variations in the optimal control trajectories versus traffic control efficiency.

On the basis of the nonlinear traffic flow model (15), the constraints (1), (2), and the cost criterion (16), a (dynamic) NOC problem is formulated over a time-horizon K, starting with the known initial state $\mathbf{x}(0)$ in the state equation (15). This NOC problem may be solved numerically in about one CPU-minute even for large-scale networks and long time-horizons by use of a feasible-direction algorithm that will be outlined in the next sections.

4.3.2 The discrete-time optimal control problem

The general discrete-time formulation of the optimal control problem reads

$$\text{Minimize} \quad \mathcal{J} = \vartheta\left[\mathbf{x}(K)\right] + \sum_{k=0}^{K-1} \varphi\left[\mathbf{x}(k), \mathbf{u}(\kappa), \mathbf{d}(k)\right] \tag{17}$$

$$\text{subject to} \quad \mathbf{x}(k+1) = \mathbf{f}[\mathbf{x}(k), \mathbf{u}(\kappa), \mathbf{d}(k)], \quad \mathbf{x}(0) = \mathbf{x}_0 \tag{18}$$

$$\mathbf{h}_1\left[\mathbf{u}(\kappa)\right] = \overline{\mathbf{A}}\mathbf{u}(\kappa) - \mathbf{b} = \mathbf{0} \tag{19}$$

$$\mathbf{h}_2\left[\mathbf{u}(\kappa)\right] = \mathbf{u}_{\min} - \mathbf{u}(\kappa) \leq \mathbf{0} \tag{20}$$

where $\mathbf{x} \in \mathbb{R}^n$ is the state vector, $\mathbf{u} \in \mathbb{R}^m$ is the control vector, and $k = 0, 1, \ldots, K-1$, $\kappa = [k/\tau]$ are the discrete-time indices of the state and control variables, respectively. The cost functional (17) expresses the control objectives in mathematical terms, whereby θ, φ are smooth, nonlinear cost functions. The state equation (18), with known initial state $\mathbf{x}_0$, describes the nonlinear dynamics of the system, while $\mathbf{d}$ is the disturbance vector which

is assumed to be known over the optimization horizon. Equations (19), (20) express the control constraints (1) and (2), respectively, whereby $\overline{\mathbf{A}} \in \mathbb{R}^{|J| \times m}$ is a sparse and separable matrix consisting of 1's and 0's reflecting the left-hand side of the constraints (1) while $b_j = C - L_j$, $j = 1, \ldots, |J|$.

The necessary conditions of (local) optimality for problem (17)–(20) are expressed in terms of the discrete-time Hamiltonian function that is defined as follows

$$\begin{aligned} \mathcal{H}[\mathbf{x}(k), \mathbf{u}(\kappa), \boldsymbol{\lambda}(k+1), \boldsymbol{\mu}(\kappa), \boldsymbol{\nu}(\kappa)] = \varphi[\mathbf{x}(k), \mathbf{u}(\kappa), \mathbf{d}(k)] + \\ + \boldsymbol{\lambda}(k+1)^T \mathbf{f}[\mathbf{x}(k), \mathbf{u}(\kappa), \mathbf{d}(k)] + \boldsymbol{\mu}(\kappa)^T \mathbf{h}_1[\mathbf{u}(\kappa)] + \boldsymbol{\nu}(\kappa)^T \mathbf{h}_2[\mathbf{u}(\kappa)] \end{aligned} \tag{21}$$

where $\boldsymbol{\lambda}(k+1) \in \mathbb{R}^n$, $\boldsymbol{\mu}(\kappa) \in \mathbb{R}^{|J|}$, and $\boldsymbol{\nu}(\kappa) \in \mathbb{R}^m$ are the Lagrange and Kuhn-Tucker multipliers for the corresponding equality and inequality constraints.

The necessary optimality conditions for a local minimum are (notation: $x_y = \partial x / \partial y$)

$$\mathcal{H}_{\boldsymbol{\lambda}(k+1)} = \mathbf{x}(k+1) = \mathbf{f}[\mathbf{x}(k), \mathbf{u}(\kappa), \mathbf{d}(k)], \quad \mathbf{x}(0) = \mathbf{x}_0 \tag{22}$$

$$\mathcal{H}_{\mathbf{x}(k)} = \boldsymbol{\lambda}(k) = \frac{\partial \varphi}{\partial \mathbf{x}(k)} + \left[\frac{\partial \mathbf{f}}{\partial \mathbf{x}(k)}\right]^T \boldsymbol{\lambda}(k+1), \quad \boldsymbol{\lambda}(K) = \vartheta_{\mathbf{x}(K)} \tag{23}$$

$$\mathcal{H}_{\mathbf{u}(\kappa)} = \sum_{k=\kappa\tau}^{(\kappa+1)\tau-1} \left\{ \frac{\partial \varphi}{\partial \mathbf{u}(\kappa)} + \left[\frac{\partial \mathbf{f}}{\partial \mathbf{u}(\kappa)}\right]^T \boldsymbol{\lambda}(k+1) \right\} + \overline{\mathbf{A}}^T \boldsymbol{\mu}(\kappa) + \left[\frac{\partial \mathbf{h}_2}{\partial \mathbf{u}(\kappa)}\right]^T \boldsymbol{\nu}(\kappa) \tag{24}$$

$$\boldsymbol{\nu}(\kappa)^T \mathbf{h}_2[\mathbf{u}(\kappa)] = 0, \quad \boldsymbol{\nu}(\kappa) \geq \mathbf{0} \tag{25}$$

$$\mathbf{h}_1[\mathbf{u}(\kappa)] = \mathbf{0}, \quad \mathbf{h}_2[\mathbf{u}(\kappa)] \leq \mathbf{0}. \tag{26}$$

Hence, if the above equations are satisfied simultaneously by some $\mathbf{x}(k+1)$, $\boldsymbol{\lambda}(k)$, $\mathbf{u}(\kappa)$, $\boldsymbol{\mu}(\kappa)$, and $\boldsymbol{\nu}(\kappa)$, $k = 0, \ldots, K-1$, a stationary point of the optimal control problem has been found.

4.3.3 A feasible-direction algorithm for numerical solution

We now describe an algorithm that can be used for the numerical solution of the discrete-time optimal control problem presented in Section 4.3.2.

The most crucial component of the solution algorithm is the calculation of appropriate feasible directions in the space of the control variables based on the problem gradients. For a given admissible trajectory $\mathbf{u}(\kappa)$, $\kappa = 0, \ldots, K_c$, where $K_c = [K/\tau] - 1$ is the control time horizon, the corresponding state trajectory $\mathbf{x}(k)$ can be found by integrating equation (22), and hence the cost criterion can be regarded as depending on the control variables only, i.e. $\mathcal{J} = \overline{\mathcal{J}}(\mathbf{u})$. The reduced gradient of $\overline{\mathcal{J}}$ with respect to $\mathbf{u}$ on the state equality constraints surface is given by

$$\mathbf{g}(\kappa) = \mathcal{H}_{\mathbf{u}(\kappa)} = \sum_{k=\kappa\tau}^{(\kappa+1)\tau-1} \left\{ \frac{\partial \varphi}{\partial \mathbf{u}(\kappa)} + \left[\frac{\partial \mathbf{f}}{\partial \mathbf{u}(\kappa)} \right]^T \boldsymbol{\lambda}(k+1) \right\} \tag{27}$$

where the co-state vector $\boldsymbol{\lambda}$ satisfies (23).

A given admissible trajectory $\mathbf{u}$ may activate a certain number q of constraints satisfying $\mathbf{h}_1 = \mathbf{0}$, $h_{2,i} = 0$, $i \in E$, while other constraints are inactive, i.e. $h_{2,i} < 0$, $i \in I$. We define the *active set* $\mathcal{A}_q$ to be the set of active constraints and $\mathbf{A}_q$ a matrix composed of the rows of active constraints. Next we seek a feasible descent direction $\mathbf{p}$ which lies in the tangent subspace defined by the active set of constraints; in the simplest case, one can project the negative gradient onto this subspace. Such a projection can be achieved by use of a symmetric projection matrix $\mathbf{P}_q$ given by (Rosen, 1960)

$$\mathbf{P}_q = \mathbf{I} - \mathbf{A}_q^T \left(\mathbf{A}_q \mathbf{A}_q^T \right)^{-1} \mathbf{A}_q. \tag{28}$$

Thus the projected gradient is given by $\boldsymbol{\gamma}(\kappa) = \mathbf{P}_q \mathbf{g}(\kappa)$.

If $\boldsymbol{\gamma}(\kappa) \neq \mathbf{0}$ then a line-search routine can be applied along the $\mathbf{p}$-direction (e.g. $\mathbf{p} = -\boldsymbol{\gamma}$) to obtain a new, improved admissible control trajectory. In the presence of constraints (19), (20) the step length α is limited by $\alpha_{\max} = \max\{\alpha \,|\, \mathbf{u} + \alpha\mathbf{p} \text{ is feasible}\}$ which represents the shortest distance to (any of) the inactive constraints, along the $\mathbf{p}$-direction.

On the other hand, if $\boldsymbol{\gamma}(\kappa) = \mathbf{0}$, the Lagrange multipliers for the active constraints are given by

$$\begin{bmatrix} \boldsymbol{\mu}(\kappa) \\ \\ \nu_{i\in E}(\kappa) \end{bmatrix} = -\left(\mathbf{A}_q \mathbf{A}_q^T\right)^{-1} \mathbf{A}_q \mathbf{g}(\kappa). \tag{29}$$

while $\nu_{i\in I}(\kappa) = 0$. In this case, if $\nu_{i\in E}(\kappa) \geq 0$ for all $i \in E$, a stationary point (in fact a local minimum) of the optimal control problem has been found since all necessary conditions for optimality (22)–(26) are satisfied. If, however, at least one of those components of $\nu_{i\in E}(\kappa)$ is negative, it is possible, by relaxing the corresponding inequality (i.e. by removing it from the active set), to specify a new direction towards an improved point. Usually, the constraint corresponding to the most negative element of $\nu_{i\in E}(\kappa)$ is the one selected to be removed. Thus, a new direction is determined by projecting the gradient onto the subspace determined by the remaining active constraints and a new iteration is started.

The solution algorithm can now be described as follows:

Step 1: Select an admissible initial control trajectory $\mathbf{u}^{(0)}(\kappa), \kappa = 0, \ldots, K_c$; set the iteration index $\ell = 0$.

Step 2: Using $\mathbf{u}^{(\ell)}(\kappa)$ solve (22) from the known initial condition to obtain $\mathbf{x}^{(\ell)}(k+1)$; using $\mathbf{x}^{(\ell)}(k+1)$ and $\mathbf{u}^{(\ell)}(\kappa)$ solve (23) from the terminal condition to obtain $\boldsymbol{\lambda}^{(\ell)}(k+1), k = 0, \ldots, K-2$.

Step 3: Using $\mathbf{x}^{(\ell)}(k+1)$, $\mathbf{u}^{(\ell)}(\kappa)$, and $\boldsymbol{\lambda}^{(\ell)}(k+1)$, calculate the reduced gradient $\mathbf{g}^{(\ell)}(\kappa)$. Find the subspace of active constraints and form $\mathcal{A}$, $\mathbf{A}_q$. Using (28) calculate the pro-

jection matrix $\mathbf{P}_q$ and the projected gradient $\boldsymbol{\gamma}^{(\ell)}(\kappa) = \mathbf{P}\mathbf{g}^{(\ell)}(\kappa)$, $\kappa = 0, \ldots, K_c$.

Step 4: Specify a search direction $\mathbf{p}^{(\ell)}(\kappa), \kappa = 0, \ldots, K_c$, e.g. steepest descent or conjugate gradients.

Step 5: Apply an one-dimensional search routine along the $\mathbf{p}^{(\ell)}$-direction to obtain a new, improved admissible control trajectory $\mathbf{u}^{(\ell+1)}(\kappa)$, i.e.

$$\alpha^{(\ell)} = \arg \min_{\alpha \in (0, \alpha_{\max}]} \overline{\mathcal{J}} \left\{ \mathbf{u}^{(\ell)}(\kappa) + \alpha \mathbf{p}^{(\ell)}(\kappa) \right\}$$

where $\alpha^{(\ell)} > 0$ is the resulting optimal admissible step length, and

$$\mathbf{u}^{(\ell+1)}(\kappa) = \mathbf{u}^{(\ell)}(\kappa) + \alpha^{(\ell)} \mathbf{p}^{(\ell)}(\kappa), \quad \forall\, \kappa = 0, \ldots, K_c.$$

Step 6: If for a given scalar $\varepsilon > 0$, the convergence condition $\|\boldsymbol{\gamma}^{(\ell)}(\kappa)\| < \varepsilon$, $\forall\, \kappa$, is not satisfied, set $\ell := \ell + 1$ and go to *Step 2*; otherwise, find the Lagrange multipliers for the active constraints from (29).

(a) If $\nu_{i \in E}(\kappa) \geq 0$ for all $i \in E$ (corresponding to active inequalities), then STOP; $\mathbf{u}(\kappa)$ satisfies the Kuhn-Tacker conditions.

(b) Otherwise, delete the row from $\mathbf{A}_q$, corresponding to the inequality with the most negative component of $\nu_{i \in E}(\kappa)$ and drop the corresponding index from $\mathcal{A}$; set $\ell := \ell + 1$ and go to *Step 2*.

At this point, it should be stressed that the constraints (19) and (20) are separable (a group of constraints at each junction) and hence the calculation of the projection matrix is computationally convenient. Moreover, since the set of active constraints in the active set changes by at most one constraint at a time, it is possible to calculate a projection matrix based on the previous one by use of a simple recursive formula (Rosen, 1960).

4.4 Discussion

We conclude this section with some remarks pertaining to some further consequences of the simplification (5) and to the application of the open-loop QPC and NOC methodologies in real time.

As a consequence of simplification (5), the updating of the control decisions cannot be effectuated more frequently than at every cycle which, however, is deemed sufficient for fast network-wide real-time control reactions; on the other hand, this feature limits the real-time communication requirements between junction controllers and the central computer to one message exchange per cycle, in contrast to the second-by-second communication requirements of other signal control systems such as SCOOT (Hunt et al., 1982).

For the application of the open-loop QPC and NOC methodologies in real time, the corresponding algorithms may be embedded in a rolling-horizon (model-predictive) scheme. More precisely, the optimal control problem may be solved on-line once per cycle using the current state (current estimates of the number of vehicles in each link) of the traffic system as the initial state as well as predicted demand flows; the optimization yields an optimal control sequence for K (or K_c) cycles, but only the first control (signal control plan) in this sequence is actually applied to the signalized junctions of the traffic network. Note that the saturation flows S_z and the turning rates $t_{w,z}$, may be assumed to be time-variant and may be estimated or predicted in real time by well-known recursive estimation schemes (Cremer, 1991); in addition, the predicted demand flows $\mathbf{d}(k)$ may be calculated by use of historical information or suitable extrapolation methods (e.g., time series or neural networks). This rolling-horizon procedure avoids myopic control actions while embedding a dynamic open-loop optimization problem in a traffic-responsive environment.

Finally, it should be stressed that, in contrast to LQ, the control decisions in QPC and

NOC methodologies are based on the explicit minimization of the cost criterion subject to all control and state constraints. Therefore, the aforementioned methodologies could be also utilized as off-line network optimization tools for calculating optimum signal control plans, since their traffic flow models (12), (15), and related constraints incorporate all necessary network characteristics.

5 A large-scale application example

To preliminarily investigate the comparative efficiency and real-time feasibility of the developed approaches to the problem of urban signal control, the urban network of the city centre of Chania, Greece, is considered. For this network, we compare the closed-loop behaviour of the linear multivariable regulator with the open-loop behaviour of QPC and NOC methodologies. To ensure fair and comparable results, all methodologies are evaluated by use of the same simulation model, namely the nonlinear traffic flow model (15) which is the most realistic among the three employed (or previously utilized) SFM versions. Although this model also includes some introduced simplifications, it is deemed quite suitable for this preliminary demonstration and comparison of methods because their respective results are more easy to compare and analyze by use of a common model that is similar in approach as the one used for their design. More sophisticated (e.g. microscopic) simulators will be used at a more advanced stage of this research in order to derive more reliable conclusions regarding the comparative method efficiencies.

5.1 Network and scenario description

The urban network of the city centre of Chania consists of 16 signalized junctions and 71 links (Fig. 4). According to the notation of Section 3, the following sets are defined:

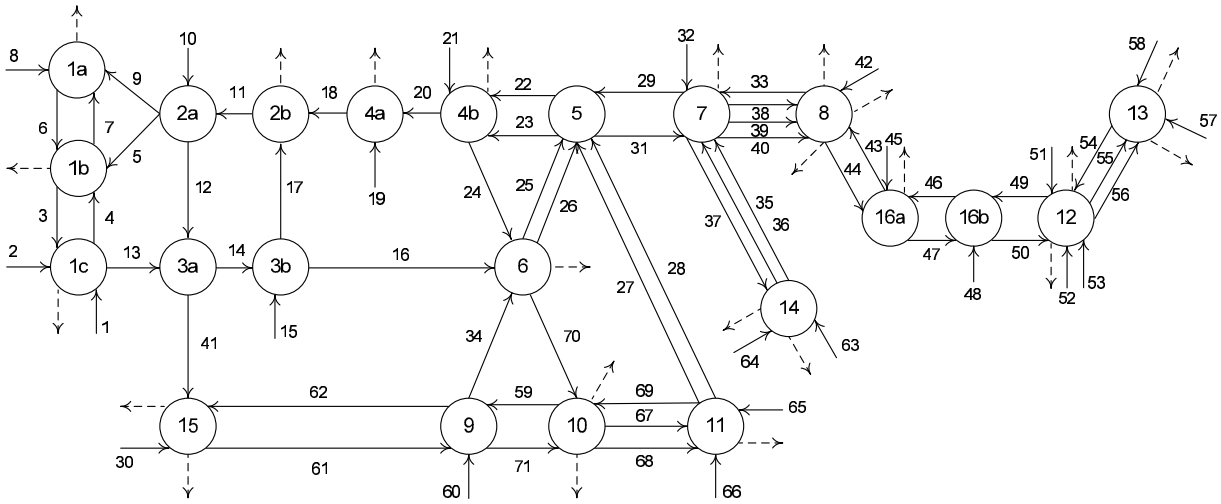

Fig. 4. The Chania urban road network.

$J = \{1, \ldots, 16\}$, $Z = \{1, \ldots, 71\}$. We omit the details on turning rates $t_{w,z}$, lost times L_j, staging v_z and saturation flows S_z. The cycle time in the network is $C = 90$ s, and $T = C$ is taken as a control interval for all strategies. For the LQ approach we consider a design parameter $r = 0.0001$ and a field-applied plan $\mathbf{g}^N$ that is not fully adapted to the traffic conditions of the test scenarios. For the NOC methodology we consider $T = 5$ s, $T_c = 90$ s, $a_f = 10^{-4}$, and $c = 0.85$ (i.e., overloaded links in (14) are considered the links z for which $x_z \geq 0.85 x_{z,\max}$).

Several tests were conducted in order to investigate the behaviour of the three alternative methodologies for different scenarios. The scenarios were created by assuming more or less high initial queues $x_z(0)$ in the origin links of the networks while the demand flows d_z were kept equal to zero. More specifically the origin link queues were selected highest for scenario 1, moderate for scenario 2, and smallest for scenario 3. The optimization horizon for each scenario is 450 s (5 cycles).

Strategy	LQ		QPC		NOC	
Scenario	TTS	RQB	TTS	RQB	TTS	RQB
1	31.1	532	30.4	445	29.9	440
2	15.2	223	13.8	183	13.2	183
3	9.3	79	8.9	63	8.8	64
Average	18.5	278	17.7	230	17.3	229.0
Improvement	-	-	-4.5%	-17.1%	-6.7%	-17.6%

Table 1
Comparison of assessment criteria.

5.2 Comparison of objective functions

For each of three distinct scenarios of initial states $\mathbf{x}(0)$ and for each control approach, two evaluation criteria were calculated for comparison. The total time spent

$$\mathrm{TTS} = T_\mathrm{c} \sum_{k=0}^{K} \sum_{z \in Z} x_z(k) \qquad (\text{in veh} \cdot \text{h})$$

and the relative queue balance

$$\mathrm{RQB} = \sum_{k=0}^{K} \sum_{z \in Z} \frac{x_z^2(k)}{x_{z,\max}} \qquad (\text{in veh}).$$

Note that, as mentioned earlier, the control results of each strategy are applied to the same nonlinear model (15). Eventually $x_z(k)$ over a whole cycle is calculated first as the average of the corresponding 5-s values resulting from (15), before applying the above criteria on the basis of $T_\mathrm{c} = C = 90$ s.

Table 1 displays the obtained results. As can be seen, QPC and NOC lead to a reduction of both evaluation criteria compared to LQ. More specifically, when QPC is applied, the TTS and RQB are improved by 4.5% and 17.1%, respectively; when NOC is applied, the TTS and RQB are improved by 6.7% and 17.6%, respectively, compared to LQ.

NOC is seen to be superior to all other strategies in terms of the TTS. This is because the nonlinear traffic flow model used by NOC is more accurate than the linear model used by

LQ or QPC (and is therefore used as a common simulator for the comparison).

Regarding the RQB, it can be seen that NOC is superior to all other strategies but is quite close to QPC. Note that RQB is the exact cost criterion considered by QPC, while in the cost criteria considered by LQ and NOC there are partially competitive subgoals (albeit with very small weights). Nevertheless, NOC maintains its superiority due to the considered nonlinear traffic flow model.

The average computational time per scenario for QPC and NOC is 10 seconds and 1 minute, respectively, which means that QPC would be feasible in a real-time rolling-horizon framework as described in Section 4.4, while for NOC, the cycle time should be higher than 1 minute for real-time feasibility.

5.3 Detailed results

In the sequel we report on some more detailed illustrative results focussing on the particular junctions 12 and 13. These two junctions carry heavy loads, since they represent a major entrance to and exit from the city centre (see Fig. 4).

For the aforementioned scenarios, the calculated optimal state and control trajectories demonstrate the efficiency of the three alternative methods to solve the urban signal control problem. Figure 5 depicts some obtained trajectories for scenario 1 for the three methods. The main observations are summarized in the following remarks:

- All strategies manage to dissolve the initial origin queues in a quite balanced way (see Figs. 5(a), 5(c), and 5(e)) and thus, the desired control objective of queue balancing is achieved. This holds particularly for origin links 52, 57, 58 (and many other origin links not shown here) that are seen to empty quasi-simultaneously; link 53 is emptied

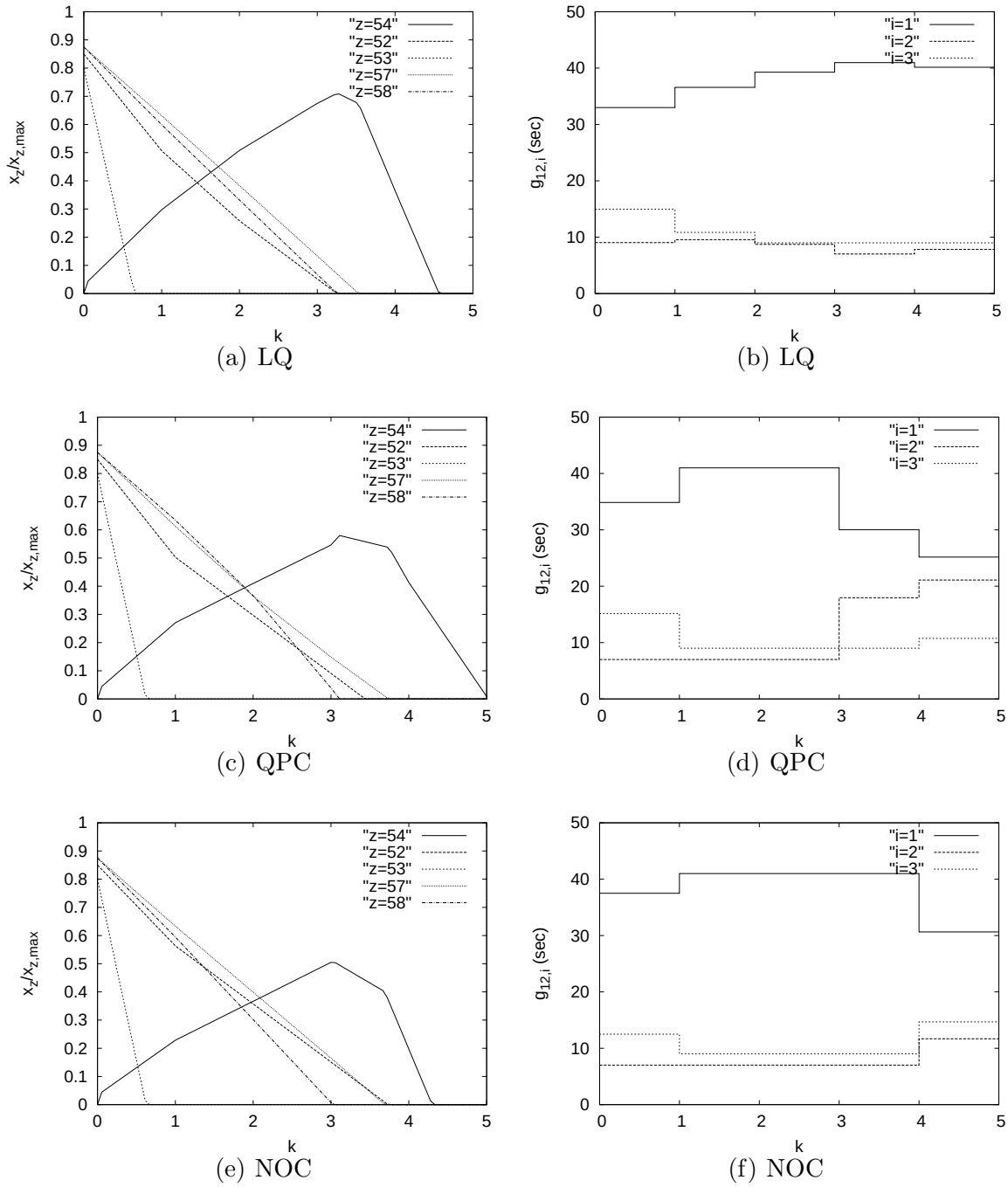

(a) LQ (b) LQ

(c) QPC (d) QPC

(e) NOC (f) NOC

Fig. 5. Relative occupancies within the links at junctions 12, 13 (LQ (a), QPC (c), NOC (e)) and the optimal green-phase durations of junction 12 (LQ (b), QPC (d), NOC (f)). Note that $g_{12,1}$ serves the internal link 54.

much faster because it receives r.o.w. at two consecutive stages; link 54 has a different behaviour because it is an internal link (see below).

- The three strategies, based on different utilized traffic flow models, accomplish the

desired goal in a very similar way.

- The outflows of the origin links 57 and 58 enter the internal link 54 (solid line in Figs. 5(a), 5(c), and 5(e)) according to the green times of the corresponding stages. It may be seen that QPC and NOC exhibit similar behaviour while managing particularly the queue of link 54 (see Figs. 5(d) and 5(f)). In contrast, the LQ strategy first allows the high initial queues to flow into the internal link 54 and then, in order to manage the developed long queue therein, it gradually increases the green time of stage 1 (see Fig. 5(b)) where link 54 has r.o.w. This somewhat slower behaviour is attributed to the infinite horizon in the LQ objective criterion (8) as opposed to the finite horizon of the QPC and NOC approaches in (13) and (16), respectively.

Both NOC and QPC deliver satisfactory results with similarly efficient control behaviour for different scenarios. Thus, taking into account that QPC needs less computational effort than NOC, QPC may be considered as a quite satisfactory method for the solution of the urban signal control problem and a strong competitor of LQ in terms of efficiency and real-time feasibility, despite the increase of real-time computation complexity.

6 Conclusions and future work

Planning new transit routes, introducing tolls in city centres, or imposing traffic restrictions are important ingredients for combating traffic congestion in urban road networks. However, it is important to supplement these policies with signal control techniques that contribute to the improvement of the traffic conditions via real-time decisions, particularly under saturation. The presented methodological framework for real-time network-wide signal control in large-scale urban traffic networks combines store-and-forward traffic flow modeling, mathematical optimization and optimal control. Clearly, the presented three alternative strategies, each with its advantages and shortcomings, can be understood as

optimal queue management tools.

Future work will deal with the comparison of the proposed open-loop QPC and NOC methodologies when embedded in a real-time rolling-horizon scheme, with other strategies (e.g. TUC) in more elaborated simulation involving external and internal demands and saturated traffic conditions as well as in real-life conditions.

Acknowledgments

This paper is part of the 03ED898 research project, implemented within the framework of the "Reinforcement Programme of Human Research Manpower" (PENED) and co-financed by National and Community Funds (75% from E.U.-European Social Fund and 25% from the Greek Ministry of Development-General Secretariat of Research and Technology).

References

Aboudolas, K., 2003. Optimal control of traffic signals in urban road networks. (in greek), M.Sc. thesis, Technical University of Crete, Chania, Greece.

Abu-Lebdeh, G., Benekohal, R. F., 1997. Development of traffic control and queue management procedures for oversaturated arterials. Transportation Research Record (1603), 119–127.

Beard, C., Ziliaskopoulos, A., 2006. A system optimal signal optimization formulation. In: Proc. of the 85th TRB Annual Meeting. Washigton, D.C., U.S.A.

Bretherton, D., Bodger, M., Baber, N., 2004. SCOOT – the future. In: Proc. of the 12th IEE International Conference on Road Transport Information and Control. London, UK, pp. 301–306.

Cremer, M., 1991. Origin-destination matrix: Dynamic estimation. In: Papageorgiou, M. (Ed.), Concise Encyclopedia of Traffic and Transportation Systems. Pergamon Press, Oxford, pp. 310–315.

Daganzo, C. F., 1994. The cell transmission model: A simple dynamic representation of highway traffic consistent with hydrodynamic theory. Transportation Research 28B (4), 269–287.

Diakaki, C., 1999. Integrated control of traffic flow in corridor road networks. Ph.D. thesis, Technical University of Crete, Chania, Greece.

Diakaki, C., Dinopoulou, V., Aboudolas, K., Papageorgiou, M., Ben-Shabat, E., Seider, E., Leibov, A., 2003. Extensions and new applications of the traffic-responsive urban control strategy: Coordinated signal control for urban networks. Transportation Research Record (1856), 202–211.

Diakaki, C., Papageorgiou, M., Aboudolas, K., 2002. A multivariable regulator approach to traffic-responsive network-wide signal control. Control Engineering Practice 10, 183–195.

Farges, J. L., Henry, J. J., Tufal, J., 1983. The PRODYN real-time traffic algorithm. In: Proc. of the 4th IFAC Symposium on Trasportation Systems. Baden-Baden, Germany, pp. 307–312.

Gartner, N. H., 1983. OPAC: A demand-responsive strategy for traffic signal control. Transportation Research Record (906), 75–84.

Gazis, D. C., Potts, R. B., 1963. The oversaturated intersection. In: Proc. of the 2nd International Symposium on Traffic Theory. London, UK, pp. 221–237.

Helgason, R., Kennington, J., Lall, H., 1980. A polynomially bounded algorithm for a singly constrained quadratic problem. Mathematical Programming 18, 338–343.

Hunt, P. B., Robertson, D. I., Bretherton, R. D., Royle, M. C., 1982. The SCOOT on-line traffic signal optimization technique. Traffic Engineering and Control 23, 190–192.

Kosmatopoulos, E., Papageorgiou, M., Bielefeldt, C., et al., 2006. International compara-

tive field evaluation of a traffic-responsive signal control strategy in three cities. Transportation Research 40A (5), 399–413.

Lo, H. K., 1999. A novel traffic signal control formulation. Transportation Research 33A (6), 433–448.

Lo, H. K., Chang, E., Chan, Y. C., 2001. Dynamic network traffic control. Transportation Research 35A (8), 721–744.

Lowrie, P. R., 1982. SCATS: The Sydney co-ordinated adaptive traffic system—Principles, methodology, algorithms. In: Proc. of the IEE International Conference on Road Traffic Signalling. London, England, pp. 67–70.

Mirchandani, P., Head, L., 1998. RHODES—A real–time traffic signal control system: Architecture, algorithms, and analysis. In: TRISTAN III (Triennial Symposium on Transportation Analysis). Vol. 2. San Juan, Puerto Rico.

Mirchandani, P., Wang, F.-Y., 2005. RHODES to intelligent transportation systems. IEEE Intelligent Systems 20 (1), 10–15.

Papageorgiou, M., 1995. An integrated control approach for traffic corridors. Transportation Research 3C (1), 19–30.

Papageorgiou, M., Diakaki, C., Dinopoulou, V., Kotsialos, A., Wang, Y., 2003. Review of road traffic control strategies. Proceedings of the IEEE 91 (12), 2043–2067.

Rosen, J. B., 1960. The gradient projection method for nonlinear programming–Part I: Linear constraints. Journal of the Society for Industrial and Applied Mathematics 8 (1), 181–217.

Schutter, B. D., Moor, B. D., 1998. Optimal traffic light control for a single intersection. European Journal of Control 4 (3), 260–276.

Singh, M. G., Tamura, H., 1974. Modelling and hierarchical optimization of oversaturated urban traffic networks. International Journal of Control 20 (6), 913–934.